Comparative study of enzymatic activities of new KatG mutants from low- and high-level isoniazid-resistant clinical isolates of Mycobacterium tuberculosis

Florence Brossier, Marlène Boudinet, Vincent Jarlier, Stéphanie Petrella, Wladimir Sougakoff

Original Article

Comparative study of enzymatic activities of new KatG mutants from low- and high-level isoniazid-resistant clinical isolates of *Mycobacterium tuberculosis*

Florence BROSSIER [a, b, *], Marlène BOUDINET [a], Vincent JARLIER [a, b], Stéphanie PETRELLA [c, d], Wladimir SOUGAKOFF [a, b]

[a] Sorbonne Universités, UPMC Univ Paris 06, CR7, INSERM, U1135, Centre d'Immunologie et des Maladies Infectieuses (CIMI), Team E13 (Bacteriology), Paris, France;

[b] AP-HP, Hôpital Pitié-Salpêtrière, Centre National de Référence des Mycobactéries et de la Résistance des Mycobactéries aux Antituberculeux (NRC MyrMA), Bactériologie-Hygiène, Paris, France.

[c] Unité de Microbiologie Structurale, Institut Pasteur, CNRS URA 2185, 25 rue du Dr Roux, Paris, France,

[d] Université Paris Diderot, Sorbonne Paris Cité (Cellule Pasteur), 25 Rue du Dr Roux, 75015 Paris, France

* Correspondence to: Florence Brossier, Laboratoire de Bactériologie-Hygiène, Faculté de Médecine, Pitié-Salpêtrière, 91 boulevard de l'Hôpital, F-75634 Paris Cedex 13, France. Phone: (+33) 1 40 77 97 46. Fax: (+33) 1 45 82 75 77. E-mail: florence.brossier@psl.aphp.fr

Abbreviations: G/Gox, glucose/glucose oxidase; IN•, isonicotinoyl acyl radical; INH, isoniazid; IN-NAD, isonicotinoyl-NAD; NBT, nitroblue tetrazolium; R, resistance; Rz, optical purity ratio of Reinheitszahl; TB, tuberculosis; tBHP, tert-butyl hydroperoxide; WT, wild-type

ABSTRACT

Resistance to isoniazid (INH-R) in *Mycobacterium tuberculosis* is mainly due to mutations at position 315 (S315T) of the catalase-peroxidase KatG. We identified 16 mutations (including 13 biochemically uncharacterized mutations) in KatG from INH-R clinical isolates of *M. tuberculosis* showing mutations other than S315T. The KatG enzymatic activities (catalase, peroxidase, free radical production and isonicotinoyl-NAD formation) of wild-type KatG and the 16 mutants were determined and correlated to their spatial location in a KatG model structure. Of all mutations studied, H270R, which conferred a high level of INH-R and results in the disruption of a coordination bond with the heme, caused complete loss of all enzymatic KatG activities. The mutants generally associated with a very high level of INH-R were all characterized by a drastic reduction in catalase activity and a marked decrease in INH activation activities. One mutant, A162E, displayed a behavior similar to S315T, i.e. a moderate decrease in catalase activity and a drastic decrease in the formation of the radical form of INH. Finally, the mutants associated with a low level of INH-R showed a moderate reduction in the four catalytic activities, likely stemming from an overall alteration of the folding and/or stability of the KatG protein.

Key words: tuberculosis, resistance, isoniazid, catalase-peroxidase, KatG, enzymatic activities

INTRODUCTION

Mycobacterium tuberculosis, the causative agent of tuberculosis, is the second leading cause of death worldwide among known infectious diseases. Isoniazid (INH), the cornerstone of front-line tuberculosis (TB) treatment, is a prodrug that needs activation by the *katG*-encoded catalase-peroxidase [1, 2]. The activated form of INH targets the NADH-dependent enoyl-acyl carrier protein reductase InhA of the fatty acid biosynthesis type II system which is involved in the synthesis of mycolic acids [3, 4]. Resistance to INH (INH-R) has been previously reported to result mainly from mutations altering the activator protein KatG (~70% of INH-R isolates have a S315T mutation in KatG) [8-10], and secondarily to mutations in the InhA protein, which prevent the activated forms of the drug to bind to the target [3, 5], and in the *inhA* promoter that cause overexpression of the target InhA [6, 7].

KatG is a heme enzyme of the class I superfamily of fungal, plant, and bacterial heme peroxidases which exhibits both high catalase activity and a broad-spectrum peroxidase activity [11, 12]. In *M. tuberculosis*, the catalase-peroxidase is responsible for activating the prodrug INH [1]. Although the details of this chemical transformation are still under investigation, it is hypothesized that INH is converted into an isonicotinoyl radical which binds to NADH/NAD^+/$NAD^\bullet$, resulting in the formation of an isonicotinoyl-NAD (IN-NAD) adduct which acts as a potent inhibitor of InhA and interferes with cell wall biosynthesis [2, 13-16].

KatG is a functional homodimer in which each monomer is composed of two domains (Figure 1). The N-terminal domain contains a heme binding site in which the heme is surrounded by a proximal pocket (made up in part by His270 and Trp321 in Figures 1 and 2A) and a distal pocket (Trp107 and His108 in Figures 1 and 2A). A peculiar structural feature unique to KatG enzymes is the presence of two covalent bonds bridging the side chains of amino acids Trp107, Tyr229 and Met255 in the distal pocket, which is required for the catalase but not the peroxidase activity [17-20]. The KatG heme is accessible to solvent through a narrow channel connecting the distal heme pocket to the outside of the protein. This pocket, which is bordered by amino acid Ser315 and filled by a network of organised water molecules (in cyan in Figures 1, 2A and 2B), has been shown to bind one INH molecule in the crystallographic structures of various KatG enzymes in complex with INH (NIZ-803 in Figures 2A and 2B) [17, 21-23]. Other potential INH binding sites, although remote from the heme, have been reported in various KatG enzymes, such as NIZ-802 and NIZ-804 from *Synechococcus elongatus* and NIZ 749 from *Burkholderia pseudomallei* (Figures 1 and 2B) [24, 25].

At the kinetic level, KatG belongs to the class I family of peroxidases [7] and is thus capable of utilizing either hydrogen peroxide or alkyl hydroperoxides to catalyze the oxidation of various substrates, including INH, via high-valent intermediates such as the oxoferryl porphyrin π-cation radical, [KatG Por^{+}•-FeIV=O] and the ferric heme coupled with a protein radical in KatG, [KatG• Por-FeIII]~~)~~ generally referred to as compounds I and II, respectively [21, 22, 26-28]. In this pathway, the two intermediate compounds I/II of KatG that are produced by oxidation of the enzyme with peroxides, can oxidize each one molecule of INH before returning to the resting state [19, 26, 29, 30]. Additional pathways have been suggested to be involved in the activation process of INH, in which the superoxide moiety, O_2•-, would be involved in the formation of the IN-NAD adduct from a ferric-superoxo form of KatG termed compound III ([KatG Por-FeIII-$O_2^{\bullet-}$]) [31, 32].

In *M. tuberculosis*, INH-R is mainly due to the presence of a mutation in the *katG* gene leading to the replacement of Ser315 by a threonine. The substitution S315T has been previously suggested to modify the main INH binding site which is located on the edge of the narrow funnel-shaped cavity leading to the heme (corresponding to NIZ-803 in Figures 2A and 2B). In fact several hypotheses have been made from the crystallographic structure of KatG S315T [28] to explain the INH-resistance of KatG S315T: a) a narrowing of the channel leading to the heme cavity conferring to the mutant KatG S315T a reduced affinity for INH, b) a reduction of water occupancy in KatG S315T which exhibits a reduced tendency to form six coordinate heme, with a less favorable binding to INH, c) an inability of oxyferrous KatG S315T to oxidize isoniazid, d) a slower turnover of INH linked to the hindrance presented by the narrower channel in Thr315, e) a disruption of the electron transfer network and f) a loss of a hydrogen bond between the side chain of S315 and a heme carboxyl group [17, 24, 28, 31-37]. The KatG mutation S315T impairs the conversion of INH to the IN-NAD adduct but preserves in part the catalase activity which is a key virulence factor in *M. tuberculosis*. The S315T substitution accounts for INH-R in ~70% of the clinical isolates of *M. tuberculosis* [6, 8, 9, 38-40]. However, in approximately 8 to 10% of the INH-R isolates, other mutations in KatG are associated with resistance by decreasing the ability of KatG to produce INH radicals, but the mechanisms by which such mutations alter the KatG activity remain partly uncharacterized.

In this study, we compare the four main enzymatic activities (catalase, peroxidase, free radical production and isonicotinoyl-NAD adduct formation) of 13 mutated proteins for which biochemical activities were never investigated, to those of the wild-type (WT) KatG enzyme of *M. tuberculosis* and three previously characterized KatG mutants, S315T [8, 9, 38, 39, 41, 42], A110V [38, 41, 42] and R463L [38, 41-43]. To our knowledge, 8 mutants are reported here for the first time (G118D,

G121D, L141S, A162E, D189G, R249H, H270R, Q461), while 5 were previously described but not studied at the enzymatic level (G494D [38], R595STOP [38], F658V [38], L336P [9], W341G [38]).

MATERIALS AND METHODS

Clinical isolates

The *M. tuberculosis* isolates were isolated at the National Reference Centre (NRC) for Mycobacteria from TB cases diagnosed in France. They were selected on the basis of their INH-R with (i) a mutation in KatG outside codon 315 and (ii) no mutation in the other genes known to be involved in INH-R (*fabG1-inhA* operon and its upstream region, *furA* and its upstream region, *ndh*), except for the KatG A110V mutant with a -15C→T mutation in the *inhA* promoter. In this study, *katG*, *fabG1-inhA* operon and its upstream region, *furA* and its upstream region, and *ndh* were amplified and sequenced as described before [38, 44, 45]. The mutations included S315T, A110V, G118D, G121D, L141S, A162E, D189G, R249H, H270R, L336P, W341G, Q461P, G494D, R595STOP and F658V detected in INH-R clinical isolates, and the polymorphism R463L found in INH-susceptible isolates. The isolates with KatG A110V, S315T, W341G, G494D, R595STOP, F658V and R463L are from previous studies [6, 38]. The others (G118D, G121D, L141S, A162E, D189G, R249H, H270R, L336P and Q461P) are from the NRC collection and have not been described before, except L336P [9]. Isolates with KatG G118D, L141S, R249H, H270R, L336P, Q461P, G494D, R595STOP were INH mono-resistant, while isolates with KatG A110V, G121D, A162E, D189G, S315T, W341G, F658V were mutidrug-resistant.

Drug susceptibility testing

Susceptibility testing was performed using the proportion method on Löwenstein-Jensen medium [46] at INH concentrations of 0.1, 0.2, 1 and 10 mg/l. A low level of resistance was defined as resistance to ≥0.2 but <1 mg/l, while a high level of resistance was defined as resistance to ≥1 mg/l of INH. In the present study we distinguished between isolates resistant to ≥1 mg/l but <10 mg/l and isolates resistant to ≥10 mg/l.

Plasmid preparation

Cloning of the *katG* gene to produce hexahistidine-tagged KatG proteins.

For KatG WT, the coding region of *katG* from H37Rv was amplified by PCR with the primers LIC1-katG (5'-GAC GAC GAC AAG ATG CCC GAG CAA CAC CCA CC-3') and LIC2-katG (5'-GAG GAG AAG CCC GGT TCA GCG CAC GTC GAA CCT-3') and cloned in the pET30 vector in NovaBlue GigaSingles™ competent *E. coli* cells using the pET-30 Ek/LIC Vector Kit (Novagen) to produce hexahistidine-tagged proteins (His_6-KatG). To obtain resistant mutants, mutagenesis was performed according to the manufacturer's protocol using the QuikChange® site-directed mutagenesis kit from Stratagene with the primers listed in Table 1. The mutated plasmids were introduced by transformation into XL1-Blue supercompetent *E. coli* cells.

Cloning of the *katG* gene to produce non-His_6-KatG proteins.

From the plasmid pET30-KatG WT, we performed site-directed mutagenesis to remove the restriction site of *Nde*I in *katG* at nucleotide 75 (Table 1). After PCR amplification of the *katG* gene with a primer containing the restriction site for *Nde*I and the 5' end of *katG* (primer KatG*Nde*I : 5'-CAT ATG CCC GAG CAA CAC C-3') and a primer containing the restriction site for *Hin*dIII and the 3' end of *katG* (primer KatG*Hin*dIII : 5'-AAG CTT TCA GCG CAC GTC G-3'), subcloning of the amplified product in TOPO was achieved with the TOPO TA cloning® kit (Invitrogen). Then, the plasmid pCR®2.1-TOPO®-KatG was digested with *Nde*I and *Hin*dIII, and the digestion product cloned into pET29 digested with the same enzymes. The ligation product was introduced into TOP-10 *E. coli* cells by electroporation.

XL1-Blue (for His_6-KatG) or TOP-10 (for non-His_6-KatG) *Escherichia coli* cells with plasmids pET30-*katG* and pET29-*katG*, respectively, were grown on Luria Bertani (LB) agar plates containing 30 µg/ml (30γ) kanamycin. Liquid cultures of LB-kanamycin 30γ were inoculated with individual colonies, grown overnight at 37°C and the bacteria pelleted by centrifugation. Plasmid DNA was extracted and purified from the bacterial pellet using the QIAprep Spin Miniprep® kit (Qiagen). Sequencing of double-stranded plasmid DNA was used to confirm the desired nucleotide substitutions and the absence of secondary mutations.

Production of the KatG proteins

The recombinant vectors pET30-His_6-*katG* and pET29-*katG* were introduced by transformation into BL-21(DE3)pLysS *E. coli* cells (Stratagene) and the cells plated onto LB-kanamycin 30γ plates and grown overnight at 37°C [31, 32]. Starter cultures (LB-kanamycin 30γ; 4 ml each) were inoculated with a single colony and grown to an optical density of 0.5-1. Each starter culture was further used to inoculate 50 ml of LB medium containing 30 mg/l hemin (dissolved in 0.2N NaOH) and 30γ kanamycin. The addition of hemin ensures stoichiometric incorporation of the heme cofactor during

overexpression in *E. coli* for maximal holoenzyme isolation [47]. For BL21 cells with pET29-*katG*, additional cultures were used to inoculate 500 ml of the same LB medium. Expression of the cloned genes was then induced with isopropyl β-D-1-thiogalactopyranoside (1 mM final concentration) and the cultures were grown overnight at 18°C. After centrifugation, the cell pellet was resuspended and lysed by sonication in an ice bucket. Cellular debris was pelleted at 18,000 x *g* for 60 min, resulting in a viscous, red-brown crude extract (except for the H270R mutant that had no color).

Purification of the catalase/peroxidase KatG

Hexahistidine-tagged KatG.

KatG proteins were purified from the crude extracts using the Ni-NTA His·Bind® resin and the His·Bind® Buffer Kit from Novagen, following the manufacturer's instructions.

Non-hexahistidine-tagged KatG

Nucleic acids were precipitated by the addition of spermine (1% w/v, final concentration) to the supernatant (15 min in ice), and the solution was centrifuged for 1 hr at 48,000 x *g* to pellet the nucleic acids. Dialysis against 20 mM Bis Tris, pH 6.0, was carried out overnight and the dialysate filtered (pore size, 0.22 µm). The clear supernatant was applied to a Q-Sepharose HiTrap™ Q HP 5 ml (GE Healthcare Life Sciences) column equilibrated with 20 mM Bis Tris, pH 6.0. The adsorbed proteins were eluted using a linear 0 to 1-M NaCl gradient. Fractions containing catalase activity, which eluted between 0.3 and 0.4 M NaCl, were pooled, dialyzed at 4°C overnight against 20 mM Bis Tris, pH 6.0, and applied to a DEAE-Sepharose (GE Healthcare Life Sciences) anion-exchange column equilibrated with Bis Tris 20 mM, pH 6.0. The adsorbed proteins were eluted using a linear 0 to 1-M NaCl gradient. The active fractions were pooled, concentrated on Amicon® Ultra filters (Millipore) and subjected to gel filtration on a Superdex™ 200 (GE Healthcare Life Sciences) column in 20 mM Bis Tris, 50 mM NaCl, pH 6.0 [11, 26, 48].

In-vitro KatG enzymatic activities

Protein concentration was determined using the heme extinction coefficient ε_{407nm} = 100 mM^{-1} cm^{-1} [28], except for the H270R mutant that contained no heme and for which the protein concentration was determined using the Bradford method with a Nanodrop® spectrophotometer (Thermo Scientific). All assays were performed in triplicate.

The catalase activity was determined spectrophotometrically by measuring the decrease in H_2O_2 concentration at 240 nm (ε_{240nm} = 0.0435 mM^{-1} cm^{-1}). The reaction mixture contained 50 mM sodium phosphate buffer, pH 7.5, 25 mM H_2O_2 and 30 nM KatG (up to 2 µM for mutants with low

catalase activity) [48, 49]. One unit (U) of catalase activity corresponded to the consumption of 1 μmole H_2O_2/min/mg of protein. The apparent K_m and k_{cat} values were obtained from non-linear regression of Michaelis-Menten [32].

The peroxidase activity was determined spectrophotometrically by measuring the rate of oxidation of 0.1 mM *O*-dianisidine, at 460 nm (ε_{460nm} = 11.3 mM^{-1} cm^{-1}) in the presence of 23 mM tert-butyl hydroperoxide (tBHP) in 50 mM sodium acetate buffer, pH 5.5 and 100 nM KatG (up to 2 μM for KatG H270R) [48, 50]. One U of peroxidase activity was defined as the oxidation of 1 mmole *O*-dianisidine/min/mg of protein.

The free radical production was followed at 560 nm using the INH-dependent reduction of nitroblue tetrazolium (NBT) to mono- and diformazan (ε_{560nm} = 15,000M^{-1} cm^{-1} for monoformazan) [49, 50]. The reaction mixture consisted of 0.2 mM NBT in 50 mM Tris HCl buffer (pH 8.5) containing INH (7.5 mM) and enzyme (30 nM, or up to 2μM for KatG H270R). The reactions were initiated by the addition of H_2O_2 (500 μM). One U of free radical production activity was defined as 1 nmole NBT reduced to monoformazan/min/nmole of heme.

The rate of isonicotinoyl-NAD (IN-NAD) adduct formation was determined spectrophotometrically at 326 nm using the extinction coefficient of isonicotinoyl-NAD (ε_{326nm} = 6.900M^{-1} cm^{-1}) [13, 28, 31, 50-52]. The reaction was carried out using KatG (2 μM), NAD+ (240 μM), the H_2O_2-generating system glucose/glucose oxidase (G/Gox) [glucose oxidase (66.6 mU/mL), glucose (16.7 mM)] [31] and INH (200 μM) in 50mM sodium phosphate, pH 7.5). The reference cuvette contained all components except NAD^+ to correct for background activity, as previously described [28, 37]. The generation of adduct was initiated by the addition of INH (200 μM). One U of isonicotinoyl-NAD formation activity was defined as the production of 1 nmole isonicotinoyl-NAD/min/nmole of heme.

Three-dimensional modeling

The location of the mutations detected in KatG was investigated using the crystal structure of the *M. tuberculosis* KatG protein (PDB entry 2CCA) [28] with PyMol software [53].

Nucleotide sequence accession numbers.

The nucleotide sequences determined for the *katG* mutants were deposited in the GenBank database under accession numbers **KC122363** to **KC122378**.

RESULTS

Purification of KatG proteins

In this study, two non-His_6-KatG proteins (KatG WT and the S315T mutant) and 17 His_6-KatG proteins (KatG WT, the S315T mutant, the polymorphism R463L mutant, and 14 other KatG mutants) were produced. The His_6-tag was introduced to facilitate the purification of the protein by nickel affinity chromatography, and the two non-His_6-KatG proteins, KatG WT and the S315T mutant, were purified in order to verify that the presence of the His_6-tag did not alter the biochemical and the enzymatic properties of KatG. The two non-tagged proteins had an optical purity ratio (Reinheitszahl: Rz) (heme Soret absorbance/total protein absorbance: A_{408}/A_{280}) [54] of 0.58 and 0.55, respectively and were obtained with typical yields of ~6 mg per liter of culture. They displayed a single band of ~80,000 daltons on SDS-PAGE, and of ~160,000 daltons on non-denaturing PAGE (data not shown). The His_6-KatG proteins were purified using immobilized metal affinity chromatography which yielded brown protein solutions with an Rz>0.5, except for the colorless KatG H270R mutant for which Rz was <0.01. The typical yield of purified protein was ~25 mg per 100 ml of culture, except for the two mutants R595STOP and Q461P for which 2 mg of protein were obtained. All mutant proteins had an apparent molecular weight of ~80,000 daltons on SDS-PAGE, except R595STOP with ~65,000 daltons (data not shown).

Enzymatic activities

Before studying the enzymatic activities of the KatG mutants, we tested whether the His_6-tag introduced to facilitate the purification of the proteins affected these activities. The K_m and k_{cat} values for catalase activity of His_6-KatG WT were nearly identical to those of non-tagged KatG WT (~10 mM and ~4.000 s^{-1}, respectively). These values were in accordance with previously reported values, ranging from 0.6 to 30 mM and from 2,300 to 10,000 s^{-1}, respectively [11, 31, 32, 48, 49, 54-56]. We also comparatively assayed for the WT and the S315T mutant the catalase and peroxidase activities, free radical production and IN-NAD adduct formation of the His_6- and non-His_6-KatG proteins which yielded very similar values (Table 2).

The catalase activity of the His_6-KatG WT enzyme was 2023±58 U and its peroxidase activity was 0.91±0.03 U. As for free radical production (NBT reduction), we noted a significant background activity of NBT reduction in the absence of isoniazid with the WT enzyme. However, NBT reduction was substantially enhanced in the presence of isoniazid, allowing us to determine after subtraction of the background activity [43, 56] the net INH-dependent reduction of NBT (free

radical production) which was 2.01±0.15 U (Table 2). Finally, isonicotinoyl-NAD adduct formation in the absence of KatG was undetectable with the H_2O_2-generating G/Gox system (data not shown) [31]. This adduct formation by His_6-KatG WT was 0.78±0.02, consistent with previously reported values [33, 37, 50, 57].

Fifteen KatG mutants from INH-R clinical isolates and the R463L mutant found in INH-susceptible clinical isolates (R463L is a phenotypically silent polymorphism) were studied comparatively to the WT enzyme (Table 2). As mentioned above, 8 have never been reported before (G118D, G121D, L141S, A162E, D189G, R249H, H270R, Q461), 5 were previously described but not studied (G494D [38], R595STOP [38], F658V [38], L336P [9], W341G [38]) and 3 were reported and their biochemical activities were investigated (S315T [8, 9, 38, 39, 41, 42], A110V [38, 41, 42], R463L [38, 41-43]). Here we report their enzymatic activities relative to those of KatG WT. The 16 KatG mutants could be categorized into six distinct groups based on the activity profiles given in Table 2. First, H270R, which was purified from a very high-level INH-R clinical isolate, was the only mutant for which no enzymatic activity was detectable (Table 2). The second group included five mutants (R595STOP, L336P, W341G, G118D, L141S) obtained from very high-level INH-R isolates and one mutant (G121D) from a high-level INH-R isolate. Overall, the six mutants were characterized by a drastic decrease in their enzymatic activities. Catalase activity was virtually undetectable in four (R595STOP, L336P, W341G and G118D), while the remaining two mutants (G121D and L141S) had very low residual activity (i.e. 14 and 2% of the KatG WT activity, respectively) (Table 2). Concomitantly, the six mutants displayed a marked alteration of free radical production activity, with values ranging from 7 to 19% (Table 2). On the other hand, the mutants, which were all impaired in their peroxidase activity and their capacity to form IN-NAD adducts, retained significant residual activities ranging from 21 to 45% for the peroxidase activity, and from 12 to 41% for the IN-NAD formation (Table 2).

The third group included two mutants, S315T and A162E, from high-level and very high-level INH-R isolates, respectively. Both were characterized by a sharp decrease in free radical production efficiency (residual activities of 9 and 26%, respectively) but were only moderately affected in their catalase and peroxidase activities (55 and 70% and 70 and 118%, respectively). S315T displayed a drastic decrease in IN-NAD formation activity (10%), while A162E appeared to be less affected (56%).

Five mutants were included in the fourth group. One of them (G494D) was identified in a high-level INH-R isolate, and four (Q461P, D189G, R249H, and F658V) were found in low-level INH-R isolates (Table 2). Overall, these five mutants showed moderately impaired enzymatic activities

when compared to the abovementioned mutants, with values ranging from 43 to 83% for catalase activity, 45 to 88% for free radical production, 72 to 109% for peroxidase activity, and 60 to 78% for IN-NAD formation (Table 2).

KatG mutant A110V was considered to form a group of its own because it showed moderately decreased catalase and free radical production activities (71 and 73%, respectively) while its peroxidase activity was markedly increased (198% compared to KatG WT). This mutant was obtained from a low-level INH-R isolate (Table 2).

Finally, mutant R463L, obtained from an INH-susceptible clinical isolate, represented a phenotypically silent polymorphism that can be found in INH-susceptible and INH-R isolates [38, 55]. When compared to KatG WT, R463L showed no variation in free radical production and the three other activities were only slightly lower (Table 2).

DISCUSSION

Analysis of the enzymatic parameters allowed the distinction of several categories of mutants that are discussed below (Table 3).

Mutants with no detectable enzymatic activity

All enzymatic activities of the KatG mutant H270R found in a very high-level INH-R isolate were abolished. The histidine residue at position 270 of KatG WT is located in the proximal pocket and forms an essential link of coordination with the iron of the heme (Figure, 2A). In the H270R protein, the mutation creates a steric hindrance and causes loss of the coordination link to the heme. Consequently, the heme cannot bind to KatG, as demonstrated by the Rz value <0.01 found for the purified H270R protein. This heme defect in KatG accounts for the complete loss of enzymatic activity of the H270R mutant.

Mutants with drastically decreased catalase and free radical production activities

The KatG R595STOP mutation, associated with a very high level of INH-R, creates a truncated protein in which 145 amino acid residues are deleted in the C-terminal domain (shown in orange in Figure 1). The yield of purification of the His_6-KatG R595STOP protein was lower than those obtained for the other proteins (2 mg versus 25 mg, respectively), indicating that the folding and/or the stability of the C-terminally truncated protein could be markedly altered. Nevertheless, the Rz value of >0.5 indicated that there is no alteration of heme binding in the active site. The catalase

activity of the R595STOP mutant was completely abolished, showing that the C-terminal region is important for this activity, even if it is generally considered to make no direct contribution to the catalytic mechanism [58]. By contrast, this mutant exhibited drastically reduced but still measurable peroxidase, free radical production and IN-NAD formation activities (Table 2), indicating that secondary oxido-reduction pathways decoupled from the catalase mechanism are still functional in the mutant protein, as previously suggested [11, 17, 31, 55].

The two mutants W341G and L336P were characterized by undetectable catalase activity and drastically reduced free-radical production activity (Table 2). They also displayed significant reduction in their peroxidase and IN-NAD formation activities. The two residues are located in the proximal pocket in the vicinity of Met377 (mean distance of ~4.1 Å) (Figure 2A) which is at 3.9 Å to Trp321 in the essential triad His270, Trp321, Asp381 (Figure 2A). Previous studies have shown that mutations in the 3 latter amino acids of the proximal triad of KatG in different bacteria are generally shown to be responsible for less than 0.1% catalase activity compared to the WT enzyme [42, 59]. In the 2 mutants W341G and L336P, which are both drastically affected in their catalase activity, the replacement of Trp341 by a glycine creates a cavity exposing Met377 to the solvent, while the introduction of a proline at position 336 probably alters the folding of the alpha-helix holding this residue and generates more room around Met377. As a consequence, both mutations induce critical structural alterations in a region essential for the catalase activity of KatG and the formation of compound I [KatG Por^{+}•FeIV=O] required for the oxidation of INH to IN•.

G118D and G121D are above the distal pocket containing the essential catalytic residue His108 (Figure 2B). Both mutants were associated with high to very high levels of INH-R and had very similar enzymatic properties with a dramatic decrease in catalase and free radical production activities (Table 2). In the 3D structure of KatG, Gly118 and Gly121 are localized at the solvent-exposed face of a long tunnel constituting the back door entrance of the distal pocket connecting the catalytic residue His108 to the outside of the protein, which contains an extended network of hydrogen-bonded water molecules and could be an equivalent of the access channel of H_2O_2 in the mono-functional catalases (Figure 2B). In both mutants, the replacement of Gly118 and Gly121 by an aspartic acid could disrupt the integrity of this channel by creating steric clashes and possibly electrostatic interactions with the side chains of two neighbouring arginine residues, Arg484 (with Asp118) and Arg418 (with Asp121) (Figure 2B), the latter acting like a catalytic switch that can be oriented toward the solvent or toward the essential Met255-Tyr229-Trp107 triad (see the two orientations in Figure 2B) [60]. One can note that G118D and G121D mutants maintained a significant level of peroxidase activity, while the catalase activity was very low (Table 2),

suggesting that oxidation of the heme by tBHP involves oxydo-reduction pathways distinct from those involved during H_2O_2 oxidation.

The L141S mutant, which was detected in a very high-level INH-R isolate, displays an extremely low level of catalase activity and a drastic reduction of free radical and IN-NAD production. Leu141 is located next to the distal pocket at a close distance (3.8 Å) to the ring of the key catalytic residue His108 (Figure 2B). It is therefore likely that Leu141 prevents the side chain of His108 to move away from the iron atom and the Trp107-Tyr229-Met255 triad which participates in the stabilization of the radical formed after initial oxidation by H_2O_2. The replacement of Leu141 by a serine not only creates room allowing His108 to shift from its optimal position, but also introduces a polar side chain in the heme region that may disturb the electron transfer pathways required for the catalase activity. Of note is the fact that the mutant displayed a significant level of peroxidase activity like the other mutants described above.

Mutants with drastically decreased free radical production activity but retaining significant catalase/peroxidase activity

Mutants S315T and A162E, which were respectively found in isolates with high- and very high-levels of INH-R displayed a unique enzymatic behaviour in the sense that there is a marked decoupling in both mutants between the catalase and peroxidase activities, which decreased slightly, and the activities of IN• production and formation of the IN-NAD adduct which decreased sharply (Table 2).

S315T, which is the most commonly occurring mutation in clinical isolates (found in ~70% of INH-R isolates), has been extensively studied in the past. In concordance with previous reports [28, 31, 32, 41, 49, 54], we observed that S315T showed a moderate reduction in catalase and peroxidase activities, contrasting with the dramatic reduction in IN• and IN-NAD formation activities (Table 2), indicating that S315T specifically affects the binding and/or processing of INH. Accordingly, S315T is located in the immediate vicinity of the heme, in the narrowest part of a short funnel-shaped channel connecting the heme pocket filled with water molecules (in cyan on Figure 2B) to the outside of the protein. This channel has been previously suggested to contain the primary INH biding site (NIZ-803 on Figure 2B) and the bulkier side chain of Thr315 would impede the access of INH to the heme pocket [28]. This model readily explains the decoupling of the effects observed for the catalase/peroxidase activities on one hand, which are in part preserved, and the loss of activation of INH on the other. However, one has to note here that alternative hypotheses have been

proposed which relate the Ser315 mutation to structural alterations affecting the porphyrin moiety and the electron transfer processes (as detailed in the Introduction section) [17, 24, 28, 31-37].

The behaviour of the A162E mutant is more puzzling. In the structure of KatG, Ala162 is located at the N-terminal part of an alpha-helix, at a very long distance to the heme pocket (Figure 2B). The side chain of Glu162, which lies very close to the solvent-exposed face of the long tunnel leading to the distal pocket, creates steric clashes with nearby residues, in particular Gly123 and Gly124 located downstream of Gly118-Gly121. It is therefore conceivable that the mutation A162E decreases the rate of free radical production (Table 2), as observed in the 2 mutants G118D and G121D. On the other hand, the limited effects observed on the catalase and peroxidase activities, are more difficult to explain.

Mutants showing moderately decreased enzymatic activities

We studied five mutants (G494D, Q461P, D189G, R249H, and F658V) that were associated with low-level of INH-R (except G494D found in a high-level resistant isolate) and that had similar catalytic effects, i.e. a moderate (G494D, Q461P and D189G) to weak (R249H and F658V) overall reduction of all measured activities that decreased within the range of 6 to 57% (Table 2). In the KatG structure, the mutated residues are remote from the heme active site, except R249H which is found in the middle of an alpha-helix located at the edge of the heme pocket (Figure 1). Despite its critical position with respect to the heme, the replacement of Arg249 by an histidine has limited impact on the enzymatic activities of KatG (Table 2), probably because the corresponding side chain is oriented toward the solvent (Figure 1). The four remaining mutations, G494D, Q461P, D189G and F658V are distant from the heme pocket, G494D, Q461P and F658V being located in the C-terminal domain of KatG (Figure 1). Interestingly, the purification yield of the Q461P mutant was significantly lower when compared to that of the other proteins (2 mg versus ca 25 mg, respectively), suggesting that the introduction of a proline at position 461 significantly impairs the folding and/or the stability of KatG. In contrast, the replacements in the 3 remaining mutants did not modify the purification yield or the Rz value. Nevertheless, the mutations gave rise to an overall impairment of the enzymatic activities (by ~50%) which may be ascribed to steric effects (F658V) and/or to modifications of ionic and polar contacts with neighboring residues (G494D and D189G).

Mutants displaying a moderate effect on catalase and INH activation, with an increased peroxidase activity

The A110V mutant was obtained from a low-level INH-R isolate, which also harboured a -15C→T mutation in the *inhA* promoter known to confer a low-level of INH-R. It is therefore difficult to establish the contribution of the KatG A110V mutation in the INH-R of this isolate [6, 7]. The residue Ala110 is located at the level of the heme pocket, not far from the catalytic residue His108 and the Trp107 of the Met255-Tyr229-Trp107 adduct (Figure 2B). Although inexplicable at the molecular level at the present state of our knowledge, our kinetic results are consistent with published observations [17, 40, 56] and confirm that the bulkier side chain of Val110 restricts the degree of freedom of the helix bearing His108, which moderately reduces the catalase and the IN• and IN-NAD formation activities (Table 2), but increases by 2 fold the peroxidase activity compared to that of WT KatG. Additionally, they confirm that there is decoupling of enzymatic functions in KatG.

Mutants that do not modify the free radical production activity and do not confer INH-R

The R463L mutation is frequently detected in INH-susceptible isolates. The residue is located far away from the porphyrin ring (56 Å) (Figure 1). As shown by our enzymatic measurements, this mutation has a very limited impact on the four enzymatic activities (Table 2). These results are consistent with published data and with the view that this mutation is an instance of a phenotypically silent polymorphism [31, 41, 54, 55].

CONCLUSION

Considering the current state of our knowledge, reaching a comprehensive understanding of the role of KatG mutations in the enzymatic perturbations observed in KatG remains a demanding task. Concluding from the observations made with the mutations identified in high-level INH-R isolates (Table 3), 7 mutants from very high-level (H270R, R595STOP, L336P, W341G, G118D, and L141S) or high-level (G121D) INH-R showed a drastic decrease in their catalase activity, resulting in the impairment of compound I [KatG Por^{+}•-FeIV=O] formation in the presence of hydrogen peroxide. As a consequence, the rate of IN• production in the presence of H_2O_2 (i.e. free radical production), which requires the formation of compound I, is dramatically affected when catalase activity is lost. However, one can note that these mutants generally retained significant peroxidase activity, an observation which sustains the hypothesis that oxidation of the heme in KatG would occur through two distinct routes according to the type of oxidizing molecule used in the reaction, i.e. the H_2O_2 pathway on one hand and the alkyl peroxide pathway (tBHP in this study) on the

other. Two other mutants from high- or very high-level INH-R isolates (S315T and A162E, respectively) exhibited an optimal balance between drastic decrease in free radical production and relative conservation of catalase and peroxidase activities, a property that may confer a survival advantage to the bacterial cell and that has been suggested previously to account for the global spread of isolates with the KatG S315T mutation [61]. Conversely, the mutants associated with low-level of INH-R, such as Q461P, D189G, R249H and F658V, were generally characterized by a moderate reduction in the four catalytic activities. Finally, it is worth highlighting that there was no strict correlation between the level of INH-R and the IN-NAD activities of the KatG mutants in our study, in accordance with previous reports [31]. However, the mutants from high- (HL1) to very high-level (HL10) INH-R isolates displayed relative activities below 50%, while those from low-level resistant isolates had relative activities above that value (Table 2).

ACKNOWLEDGMENTS

We gratefully acknowledge Nicolas Veziris who provided us with the isolates and Anabella Ivancich for helpful discussions. We thank Ekkehard Collatz for English editing.

COMPETING INTERESTS

None declared.

FUNDING

This work was supported by grants from the Institut National de la Santé et de la Recherche Médicale (INSERM) and the Université Pierre et Marie Curie (UPMC).

ETHICAL APPROVAL

Not required.

REFERENCES

[1] Zhang Y, Heym B, Allen B, Young D, Cole S. The catalase peroxidase gene and isoniazid resistance of *Mycobacterium tuberculosis*. Nature 1992;358:591-3.

[2] Johnsson K, Schultz PG. Mechanistic studies of the oxidation of isoniazid by the catalase peroxidase from *Mycobacterium tuberculosis*. J Am Chem Soc 1994;116:7425-6.

[3] Banerjee A, Dubnau E, Quemard A, Balasubramanian V, Um KS, Wilson T, et al. *inhA*, a gene encoding a target for isoniazid and ethionamide in *Mycobacterium tuberculosis*. Science 1994;263:227-30.

[4] Marrakchi H, Laneelle G, Quemard A. InhA, a target of the antituberculous drug isoniazid, is involved in a mycobacterial fatty acid elongation system, FAS-II. Microbiology 2000;146**:**289-96.

[5] Vilchèze C, Wang F, Arai M, Hazbon MH, Colangeli R, Kremer L, et al. Transfer of a point mutation in *Mycobacterium tuberculosis inhA* resolves the target of isoniazid. Nat Med 2006;12:1027-9.

[6] Brossier F, Veziris N, Jarlier V, Sougakoff W. Performance of MTBDR plus for detecting high/low levels of *Mycobacterium tuberculosis* resistance to isoniazid. Int J Tuberc Lung Dis 2009;13:260-5.

[7] Larsen MH, Vilcheze C, Kremer L, Besra GS, Parsons L, Salfinger M, et al. Overexpression of *inhA*, but not *kasA*, confers resistance to isoniazid and ethionamide in *Mycobacterium smegmatis*, *M. bovis* BCG and *M. tuberculosis*. Mol Microbiol 2002;46:453-66.

[8] Hazbón MH, Brimacombe M, Bobadilla del Valle M, Cavatore M, Guerrero MI, Varma-Basil M, et al. Population genetics study of isoniazid resistance mutations and evolution of multidrug-resistant *Mycobacterium tuberculosis*. Antimicrob Agents Chemother 2006;50:2640-9.

[9] Ramaswamy SV, Reich R, Dou SJ, Jasperse L, Pan X, Wanger A, et al. Single nucleotide polymorphisms in genes associated with isoniazid resistance in *Mycobacterium tuberculosis*. Antimicrob Agents Chemother 2003;47:1241-50.

[10] Zhang Y. Isoniazid. In: Rom WN, Garay SM, editors. Tuberculosis. 2nd ed. Philadelphia, PA, USA: Lippincott Williams and Wilkins; 2004, p. 739-758.

[11] Nagy JM, Cass AE, Brown KA. Purification and characterization of recombinant catalase-peroxidase, which confers isoniazid sensitivity in *Mycobacterium tuberculosis*. J Biol Chem 1997;272:31265-71.

[12] Welinder KG. Bacterial catalase-peroxidases are gene duplicated members of the plant peroxidase superfamily. Biochim Biophys Acta 1991;1080:215-20.

[13] Lei B, Wei CJ, Tu SC. Action mechanism of antitubercular isoniazid. Activation by *Mycobacterium tuberculosis* KatG, isolation, and characterization of InhA inhibitor. J Biol Chem 2000;275:2520-6.

[14] Quémard A, Sacchettini JC, Dessen A, Vilcheze C, Bittman R, Jacobs WR Jr, et al. Enzymatic characterization of the target for isoniazid in *Mycobacterium tuberculosis*. Biochemistry 1995;34:8235-41.

[15] Rozwarski DA, Grant GA, Barton DH, Jacobs WR Jr, Sacchettini JC. Modification of the NADH of the isoniazid target (InhA) from *Mycobacterium tuberculosis*. Science 1998;279:98-102.

[16] Vilchèze C, Jacobs WR Jr. The mechanism of isoniazid killing: clarity through the scope of genetics. Annu Rev Microbiol 2007;61:35-50.

[17] Bertrand T, Eady NA, Jones JN, Jesmin, Nagy JM, Jamart-Grégoire B, et al. Crystal structure of *Mycobacterium tuberculosis* catalase-peroxidase. J Biol Chem 2004;279:38991-9.

[18] Carpena X, Loprasert S, Mongkolsuk S, Switala J, Loewen PC, Fita I. Catalase-peroxidase KatG of *Burkholderia pseudomallei* at 1.7 Å resolution. J Mol Biol 2003;327:475-89.

[19] Ghiladi RA, Knudsen GM, Medzihradszky KF, Ortiz de Montellano PR. The Met-Tyr-Trp cross-link in *Mycobacterium tuberculosis* catalase-peroxidase (KatG): autocatalytic formation and effect on enzyme catalysis and spectroscopic properties. J. Biol Chem 2005;280:22651-63.

[20] Yamada Y, Fujiwara T, Sato T, Igarashi N, Tanaka N. The 2.0 Å crystal structure of catalase-peroxidase from *Haloarcula marismortui*. Nat Struct Biol 2002;9:691-5.

[21] Metcalfe C, Macdonald IK, Murphy EJ, Brown KA, Raven EL, Moody PC. The tuberculosis prodrug isoniazid bound to activating peroxidases. J Biol Chem 2008;283:6193-200.

[22] Pierattelli R, Banci L, Eady NA, Bodiguel J, Jones JN, Moody PC, et al. Enzyme-catalyzed mechanism of isoniazid activation in class I and class III peroxidases. J Biol Chem 2004;279:39000-9.

[23] Singh AK, Kumar RP, Pandey N, Singh N, Sinha M, Bhushan A, et al. Mode of binding of the tuberculosis prodrug isoniazid to heme peroxidases: binding studies and crystal structure of bovine lactoperoxidase with isoniazid at 2.7 Å resolution. J Biol Chem 2010; 285:1569-76.

[24] Wiseman B, Carpena X, Feliz M, Donald LJ, Pons M, Fita I, et al. Isonicotinic acid hydrazide conversion to isonicotinyl-NAD by catalase-peroxidases. J Biol Chem 2010;285:26662-73.

[25] Kamachi S, Hirabayashi K, Tamoi M, Shigeoka S, Tada T, Wada K. The crystal structure of isoniazid-bound KatG catalase-peroxidase from *Synechococcus elongatus* PCC7942. FEBS J 2015;282:54-64.

[26] Chouchane S, Lippai I, Magliozzo RS. Catalase-peroxidase (*Mycobacterium tuberculosis* KatG) catalysis and isoniazid activation. Biochemistry 2000 ; 39:9975-83.

[27] Magliozzo RS, Marcinkevieciene JA. Evidence for isoniazid oxidation by oxyferrous mycobacterial catalase-peroxidase. J Am Chem Soc 1996;118:11303-4.

[28] Zhao X, Yu H, Yu S, Wang F, Sacchettini JC, Magliozzo RS. Hydrogen peroxide-mediated isoniazid activation catalyzed by *Mycobacterium tuberculosis* catalase-peroxidase (KatG) and its S315T mutant. Biochemistry 2006;45:4131-40.

[29] Ghiladi RA, Medzihradszky KF, Ortiz de Montellano PR. Role of the Met-Tyr-Trp cross-link in *Mycobacterium tuberculosis* catalase-peroxidase (KatG) as revealed by KatG(M255I). Biochemistry 2005;44:15093-105.

[30] Jakopitsch C, Droghetti E, Schmuckenschlager F, Furtmüller PG, Smulevich G, Obinger C. Role of the main access channel of catalase-peroxidase in catalysis. J Biol Chem 2005;280:42411-22.

[31] Cade CE, Dlouhy AC, Medzihradszky KF, Salas-Castillo SP, Ghiladi RA. Isoniazid-resistance conferring mutations in *Mycobacterium tuberculosis* KatG: catalase, peroxidase, and INH-NADH adduct formation activities. Protein Sci 2010;19:458-74.

[32] Ghiladi RA, Medzihradszky KF, Rusnak FM, Ortiz de Montellano PR. Correlation between isoniazid resistance and superoxide reactivity in *Mycobacterium tuberculosis* KatG. J Am Chem Soc 2005;127:13428-42.

[33] Yu S, Girotto S, Lee C, Magliozzo RS. Reduced affinity for isoniazid in the S315T mutant of *Mycobacterium tuberculosis* KatG is a key factor in antibiotic resistance. J Biol Chem 2003;278:14769-75.

[34] Kapetanaki SM, Chouchane S, Girotto S, Yu S, Magliozzo RS, Schelvis JP. Conformational differences in *Mycobacterium tuberculosis* catalase-peroxidase KatG and its S315T mutant revealed by resonance raman spectroscopy. Biochemistry 2003;42:3835-45.

[35] Deemagarn T, Wiseman B, Carpena X, Ivancich A, Fita I, Loewen PC. Two alternative substrate paths for compound I formation and reduction in catalase-peroxidase KatG from *Burkholderia pseudomallei*. Proteins 2007;66:219-28.

[36] Singh R, Switala J, Loewen PC, Ivancich A. Two [Fe(IV)=O Trp*] intermediates in *M. tuberculosis* catalase-peroxidase discriminated by multifrequency (9-285 GHz) EPR spectroscopy: reactivity toward isoniazid. J Am Chem Soc 2007;29:15954-63.

[37] Suarez J, Ranguelova K, Schelvis JP, Magliozzo RS. Antibiotic resistance in *Mycobacterium tuberculosis*: peroxidase intermediate bypass causes poor isoniazid activation by the S315G mutant of *M. tuberculosis* catalase-peroxidase (KatG). J Biol Chem 2009;284:16146-55.

[38] Brossier F, Veziris N, Truffot-Pernot C, Jarlier V, Sougakoff W. Performance of the Genotype MTBDR line probe assay for detection of resistance to rifampin and isoniazid in strains of *Mycobacterium tuberculosis* with low- and high-level resistance. J Clin Microbiol 2006;44:3659-64.

[39] Cardoso RF, Cooksey RC, Morlock GP, Barco P, Cecon L, Forestiero F, et al. Screening and characterization of mutations in isoniazid-resistant *Mycobacterium tuberculosis* isolates obtained in Brazil. Antimicrob Agents Chemother 2004;48:3373-81.

[40] Musser JM, Kapur V, Williams DL, Kreiswirth BN, van Soolingen D, van Embden JD. Characterization of the catalase-peroxidase gene (*katG*) and *inhA* locus in isoniazid-resistant and -susceptible strains of *Mycobacterium tuberculosis* by automated DNA sequencing: restricted array of mutations associated with drug resistance. J Infect Dis 1996;1731:196-202.

[41] Ando H, Kondo Y, Suetake T, Toyota E, Kato S, Mori T, et al. Identification of *katG* mutations associated with high-level isoniazid resistance in *Mycobacterium tuberculosis*. Antimicrob Agents Chemother 2010;54:1793-9.

[42] Vilchèze C, Jacobs WR Jr. Resistance to isoniazid and ethionamide in *Mycobacterium tuberculosis*: genes, mutations, and causalities. Microbiol Spectr 2014;2:MGM2-0014-2013.

[43] Sekiguchi J, Miyoshi-Akiyama T, Augustynowicz-Kopeć E, Zwolska Z, Kirikae F, Toyota E, et al. Detection of multidrug resistance in *Mycobacterium tuberculosis*. J Clin Microbiol 2007;45:179-92.

[44] Pym AS, Domenech P, Honore N, Song J, Deretic V, Cole ST. Regulation of catalase-peroxidase (KatG) expression, isoniazid sensitivity and virulence by *furA* of *Mycobacterium tuberculosis*. Mol Microbiol 2001;40:879-89.

[45] Brossier F, Veziris N, Truffot-Pernot C, Jarlier V, Sougakoff W. Molecular investigation of resistance to the antituberculous drug ethionamide in multidrug-resistant clinical isolates of *Mycobacterium tuberculosis*. Antimicrob Agents Chemother 2011;55:355-60.

[46] Canetti G, Rist N, Grosset J. Measurement of sensitivity of the tuberculous bacillus to antibacillary drugs by the method of proportions. Methodology, resistance criteria, results and interpretation. Rev Tuberc Pneumol (Paris) 1963;27:217-72.

[47] Wengenack NL, Uhl JR, St Amand AL, Tomlinson AJ, Benson LM, Naylor S, et al. Recombinant *Mycobacterium tuberculosis* KatG(S315T) is a competent catalase-peroxidase with reduced activity toward isoniazid. J Infect Dis 1997;176:722-7.

[48] Marcinkeviciene JA, Magliozzo RS, Blanchard JS. Purification and characterization of the *Mycobacterium smegmatis* catalase-peroxidase involved in isoniazid activation. J Biol Chem 1995;270:22290-5.

[49] Saint-Joanis B, Souchon H, Wilming M, Johnsson K, Alzari PM, Cole ST. Use of site-directed mutagenesis to probe the structure, function and isoniazid activation of the catalase/peroxidase, KatG, from *Mycobacterium tuberculosis*. Biochem J 1999;338:753-60.

[50] Singh R, Wiseman B, Deemagarn T, Jha V, Switala J, Loewen PC. Comparative study of catalase-peroxidases (KatGs). Arch Biochem Biophys 2008;471:207-14.

[51] Rawat R, Whitty A, Tonge PJ. The isoniazid-NAD adduct is a slow, tight-binding inhibitor of InhA, the *Mycobacterium tuberculosis* enoyl reductase: adduct affinity and drug resistance. Proc Natl Acad Sci USA 2003;100:13881-6.

[52] Singh R, Wiseman B, Deemagarn T, Donald LJ, Duckworth HW, Carpena X, et al. Catalase-peroxidases (KatG) exhibit NADH oxidase activity. J Biol Chem 2004;279:43098-106.

[53] Pan L, Aller SG. Tools and procedures for visualization of proteins and other biomolecules. Curr. Protoc. Mol Biol 2015;110:19.12.1-19.12.47.

[54] Wengenack N L, Lane BD, Hill PJ, Uhl JR, Lukat-Rodgers GS, Hall L, et al. Purification and characterization of *Mycobacterium tuberculosis* KatG, KatG(S315T) and *Mycobacterium bovis* KatG(R463L). Protein Expr Purif 2004;36:232-43.

[55] Johnsson K, Froland WA, Schultz PG. Overexpression, purification, and characterization of the catalase-peroxidase KatG from *Mycobacterium tuberculosis*. J Biol Chem 1997;272:2834-40.

[56] Wei CJ, Lei B, Musser JM, Tu SC. Isoniazid activation defects in recombinant *Mycobacterium tuberculosis* catalase-peroxidase (KatG) mutants evident in InhA inhibitor production. Antimicrob. Agents Chemother 2003;47:670-5.

[57] Yu S, Chouchane S, Magliozzo RS. Characterization of the W321F mutant of *Mycobacterium tuberculosis* catalase-peroxidase KatG. Protein Sci 2002;11:58-64.

[58] Baker RD, Cook CO, Goodwin DC. Properties of catalase-peroxidase lacking its C-terminal domain. Biochem Biophys Res Commun 2004;320:833-9.

[59] Smulevich G, Jakopitsch C, Droghetti E, Obinger C. Probing the structure and bifunctionality of catalase-peroxidase (KatG). J Inorg Biochem 2006;100:568-85.

[60] Vidossich P, Alfonso-Prieto M, Carpena X, Loewen PC, Fita I, Rovira C. Versatility of the electronic structure of compound I in catalase-peroxidases. J Am Chem Soc 2007;129:13436-46.

[61] Pym AS, Saint-Joanis B, Cole ST. Effect of *katG* mutations on the virulence of *Mycobacterium tuberculosis* and the implication for transmission in humans. Infect Immun 2002;70:4955-60.

Table 1. Mutagenic primers employed in the site-directed mutagenesis of WT KatG using the QuickChange XL kit. The changed bases are in boldface.

A110V	5’-GGC GTG GCA CGC TG**T** CGG CAC CTA CCG CAT CC-3’
	3’-GG ATG CGG TAG GTG CCG **A**CA GCG TGC CAC GCC-5’
G118D	5’-CCG CAT CCA CGA CG**A** CCG CGG CGG C-3’
	5’-G CCG CCG CGG **T**CG TCG TGG ATG CGG-3’
G121D	5’-CGA CGG CCG CGG CG**A** CGC CGG GGG CGG C-3’
	3’-G CCG CCC CCG GCG **T**CG CCG CGG CCG TCG-3’
L141S	5’-CCC GAC AAC GCC AGC T**C**G GAC AAG GCG CG-3’
	5’-CG CGC CTT GTC C**G**A GCT GGC GTT GTC GGG-3’
A162E	5’-GCT CTC ATG GG**A** GGA CCT GAT TGT TTT CGC-3’
	5’-GCG AAA ACA ATC AGG TCC **T**CC CAT GAG AGC-3’
D189G	5’-GCT TCG GCC GGG TCG **G**CC AGT GGG AGC-3’
	5’-GCT CCC ACT GG**C** CGA CCC GGC CGA AGC-3’
R249H	5’-CGG CGG TCG ACA TTC **A**CG AGA CGT TTC GG-3’
	5’-CC GAA ACG TCT CG**T** GAA TGT CGA CCG CCG-3’
H270R	5’-CGT CGG CGG TC**G** CAC TTT CGG TAA GAC CC-3’
	5’-GG GTC TTA CCG AAA GTG **C**GA CCG CCG ACG-3’
S315T	5’-GGA CGC GAT CAC CA**C** CGG CAT CGA GGT CG-3’
	5’-CG ACC TCG ATG CGG **G**TG GTG ATC GCG TCC-5’
L336P	5’-CCT CGA GAT CC**C** GTA CGG CTA CGA GTG GG-3’
	5’-CC CAC TCG TAG CCG TAC **G**GG ATC TCG AGG-3’
W341G	5’-CCT GTA CGG CTA CGA G**G**G GGA GCT GAC GAA GAG CC-3’
	5’-GGC TCT TCG TCA GCT CCC **C**CT CGT AGC CGT ACA GG-3’
Q461P	5’-CCA GCC TTA AGA GCC **C**GA TCC GGG CAT CGG G-3’
	3’-C CCG ATG CCC GGA TC**G** GGC TCT TAA GGC GGT-3’
R463L	5’-GCC AGC CTT AAG AGC CAG ATC C**T**G GCA TCG GGA TTG ACT G-3’
	5’-C AGT CAA TCC CGA TGC C**A**G GAT CTG GCT CTT AAG GCT GGC-3’
G494D	5’-GGC GGC GCC AAC G**A**T GGT CGC ATC CGC CTG C-3’
	3’-G CAG GCG GAT GCG CCA A**T**C GTT GGC GCC GCC-5’
R595STOP	5’-GGC AGA TGG CTT C**T**G AAA CTA CCT CGG AAA GGG-3’

	5’-CCC TTT CCG AGG G**A**T TTT CAG AAG CCA TCT GCC-3’
F658V	5’-CAC TGA CCA ACG ACT TC**G** TCG TGA ACC TGC TCG-3’
	5’-CGA GCA GGT TCA CGA **C**GT AGT CGT TGG TCA GTG-3’
WT	5’-CCC GTC GTG GGT CA**C** [a] ATG AAA TAC CCC GTC G-5’
	5’-CGA CGG GGT ATT TCA T**G**T GAC CCA CGA CGG G-3’

[a] (nt 75: T→C)

Table 2. Enzymatic activities of KatG wild-type and 16 KatG mutants

KatG [b]	Enzymatic activity (U) [a]				Level of INH resistance[c]
	Catalase	Peroxidase	Free radical production	Isonicotinoyl-NAD formation	
WT	2023±58	0.91±0.03	2.01±0.15	0.78±0.02	S
non-His_6 WT	2225±101	0.89±0.04	2.60±0.04	0.73±0.02	S
H270R	<2 (<0.1%)	<0.01 (<0.1%)	<0.01 (<0.1%)	<0.01 (<0.1%)	R (HL10)
R595STOP	<2 (<0.1%)	0.19±0.01 (21%)	0.28±0.02 (14%)	0.09±0.02 (12%)	R (HL10)
L336P	<2 (<0.1%)	0.23±0.02 (25%)	0.38±0.04 (19%)	0.12±0.01 (15%)	R (HL10)
W341G	<2 (<0.1%)	0.31±0.03 (34%)	0.26±0.02 (13%)	0.32±0.02 (41%)	R (HL10)
G118D	<2 (<0.1%)	0.27±0.01 (30%)	0.16±0.04 (8%)	0.23±0.03 (29%)	R (HL10)
G121D	283±4 (14%)	0.40±0.01 (44%)	0.14±0.02 (7%)	0.16±0.03 (21%)	R (HL1)
L141S	40±4 (2%)	0.41±0.04 (45%)	0.28±0.10 (14%)	0.24±0.02 (31%)	R (HL10)
A162E	1416±40 (70%)	1.07±0.02 (118%)	0.52±0.06 (26%)	0.44±0.01 (56%)	R (HL10)
S315T	1112±40 (55%)	0.64±0.04 (70%)	0.18±0.02 (9%)	0.08±0.01 (10%)	R (HL1)
Non-His_6 S315T	951±121 (47%)	0.47±0.01 (52%)	0.18±0.02 (9%)	0.07±0.01 (9%)	R (HL1)
G494D	870±40 (43%)	0.65±0.02 (72%)	1.04±0.04 (52%)	0.55±0.03 (70%)	R (HL1)
Q461P	890±20 (44%)	0.53±0.01 (58%)	0.90±0.06 (45%)	0.55±0.04 (71%)	R (LL)

D189G	1072±182 (53%)	0.54±0.01 (59%)	0.98±0.08 (49%)	0.47±0.01 (60%)	R (LL)
R249H	1497±61 (74%)	0.70±0.02 (77%)	1.63±0.14 (81%)	0.54±0.02 (69%)	R (LL)
F658V	1679±40 (83%)	0.99±0.03 (109%)	1.77±0.14 (88%)	0.61±0.02 (78%)	R (LL)
A110V	1436±40 (71%)	1.80±0.02 (198%)	1.47±0.04 (73%)	0.31±0.02 (40%)	R (LL)
R463L	1598±101 (79%)	0.81±0.03 (89%)	2.05±0.06 (102%)	0.67±0.01 (86%)	S

[a] (%) = Normalized to the value obtained for WT KatG as 100%.

[b] WT= wild-type

[c] S= susceptible; R= resistant; LL= low-level resistant, defined as resistant to >0.1 but <1 mg/l of INH; HL= high-level resistant, defined as resistant to ≥1 mg/l; HL1= resistant to ≥1 mg/l but <10 mg/l; HL10= resistant to ≥10 mg/l.

Table 3. Correlation between the different classes of mutants and changes in amino acids in KatG

Classes of mutants	KatG	Location of the mutation	Level of INH resistance
Mutants with no detectable enzymatic activity	H270R	Loss of the coordination link between H270 and the iron of the heme	R (HL10)
Mutants with drastically decreased catalase and free radical production activities	R595STOP	Deletion of the C-terminal domain	R (HL10)
	W341G	In the proximal pocket, close to the proximal triad	R (HL10)
	L336P	In the proximal pocket, close to the proximal triad	R (HL10)
	G118D	In the long tunnel connecting the entrance to the distal pocket	R (HL10)
	G121D	In the long tunnel connecting the entrance to the distal pocket	R (HL1)
	L141S	Next to the distal pocket and the key catalytic residue H108	R (HL10)
Mutants with drastically decreased free radical production activity but retaining significant catalase/peroxidase activity	S315T	In the short channel connecting the heme pocket to the outside of the protein	R (HL1)
	A162E	In the long tunnel connecting the entrance to the distal pocket	R (HL10)
Mutants showing moderately decreased enzymatic activities	G494D	Remote from the heme	R (HL1)
	Q461P	Remote from the heme	R (LL)
	D189G	Remote from the heme	R (LL)
	R249H	At the edge of the heme pocket, with a solvent-exposed side-chain	R (LL)
	F658V	Remote from the heme	R (LL)
Mutants displaying a moderate effect on catalase and INH activation, with an increased peroxidase activity	A110V	At the level of the heme pocket, not far from the catalytic residue H108 and the M255-Y229-W107 adduct	R (LL)
Mutants that do not modify the free radical production activity and do not confer INH-R	R463L	Far from the heme	S

Figure 1. Three-dimensional representation (ribbon model) of KatG of *M. tuberculosis* (PDB entry 2CCA).

The heme prosthetic group and the catalytic His108 are shown in black. The mutated residues are represented using red sticks for His270, Trp341, Leu336, Leu141, Ser315, Ala162, Gln461, Asp189, Arg249, Phe658, Ala110 and Arg463, while red spheres are used to represent Gly118, Gly121 and Gly494. The segment of polypeptide chain deleted in the Arg595STOP mutant is shown in orange. The numerous tryptophan, tyrosine and methionine residues present in KatG are shown as thin blue lines. Water molecules (cyan and blue spheres) indicate the location of the two access channels to the heme: a long and wide channel (filled by water molecules represented in blue) that extends from the surface of the protein to the catalytic residue His108, and a narrower short channel connecting the distal heme pocket to the protein surface at the level of residue S315 (corresponding to the water molecules represented in cyan). The yellow INH molecules (NIZ) indicate four potential INH binding sites in KatG which have been positioned by superimposing the 3D structures of KatG of *M. tuberculosis*, *S. elongatus* and *B. pseudomallei* [24, 25, 28]. The binding site corresponding to NIZ-803, which is generally considered to be the main INH binding site in KatG, has been inferred from cristallographic structures of class I, II, III peroxidases in complex with INH or other small aromatic compounds of similar structure to INH [17, 21-23]. It is located in the narrowest part of the channel connecting the distal heme pocket to the protein surface at the level of S315, hence at the entrance to the ε-edge side of the heme [25]. Structural comparisons have revealed that the identity and configuration of the residues in the binding site corresponding to NIZ-803 are very similar among *S. elongatus* KatG, *B. pseudomallei* KatG, and *M. tuberculosis* KatG. NIZ-802 and NIZ-804 have been recently identified in KatG of *S. elongatus*, at the level of the entrance to the γ-edge side of the heme and in front of the heme propionate side chain, respectively [25], and NIZ-749 in KatG of *B. pseudomallei* at the entrance of a long channel connecting the distal pocket to the outside of the protein [24]. In contrast to the binding site corresponding to NIZ-803, the environment of NIZ-802 and NIZ-804 are structurally more diverse among the three KatG proteins of *S. elongatus*, *B. pseudomallei*, and *M. tuberculosis*. Image constructed using PyMOL [53].

Figure 2. Close-ups showing structural details in three regions of KatG.

The legend is the same as in Figure 1. **2A**, view of the mutated residues in the proximal pocket (His270, Leu336 and Trp341, in red). Trp321 (forming a transient tryptophan radical), Asp381 and Met377 are depicted as blue sticks. Distances (in Å) are indicated by black dotted lines. **2B**, view of the mutated residues in the distal pocket (Gly118, Gly121, Leu141, Ala162, Ser315, Asp189 and Ala110, in red). Two Arg residues (Arg418 and Arg484 potentially interacting with residues 118 and 121), are shown as blue sticks. The Met255-Tyr229-Trp107 adduct is visible close to His108. The two arrows indicate the opening of the two access channels. H-bonds are depicted as blue dotted lines.

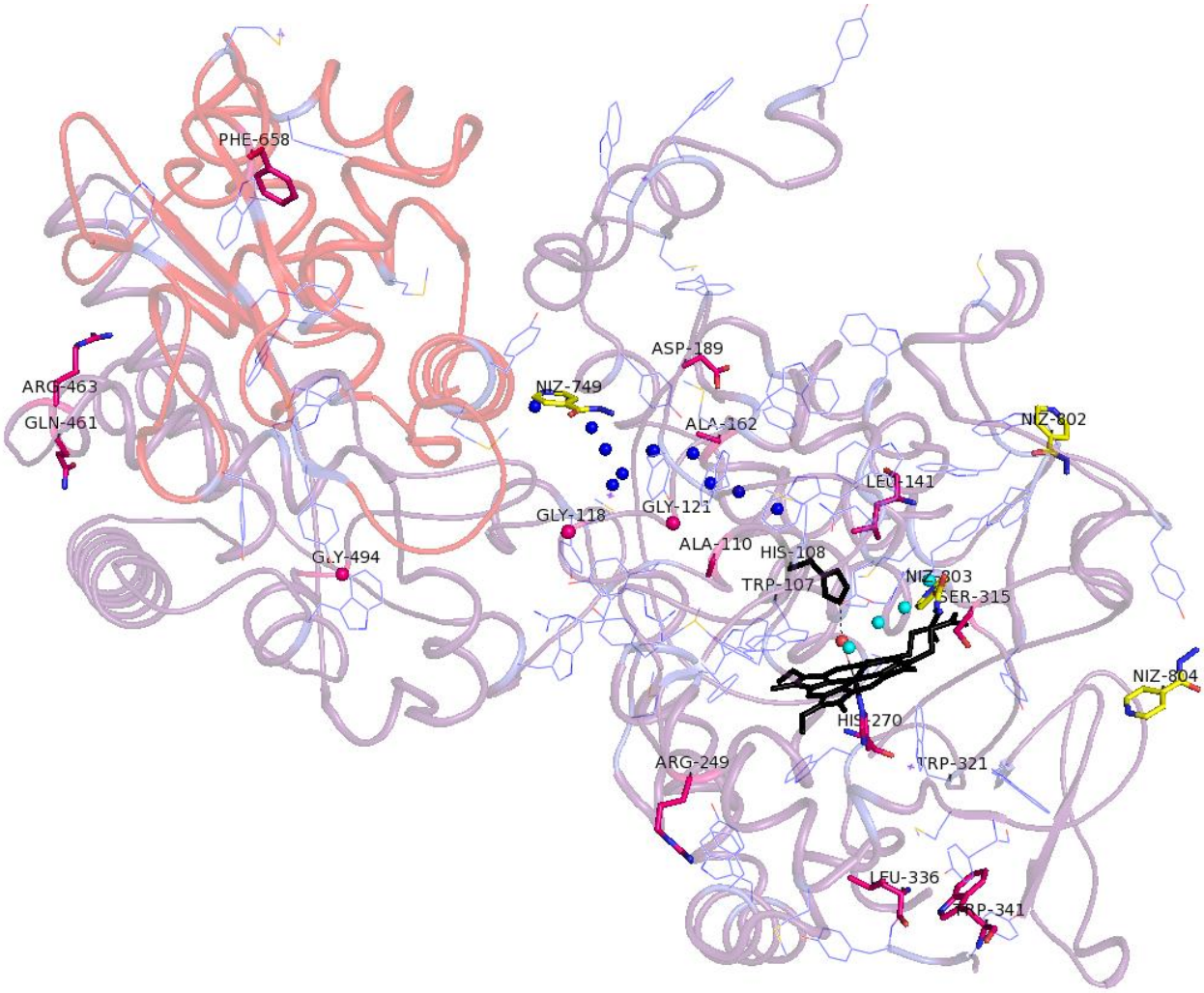
PHE-658
ARG-463
GLN-461
NIZ-749
ASP-189
ALA-162
NIZ-802
LEU-141
GLY-118
GLY-121
ALA-110
HIS-108
TRP-107
NIZ-803
SER-315
GLY-494
NIZ-804
HIS-270
ARG-249
TRP-321
LEU-336
TRP-341

Figure 1

A

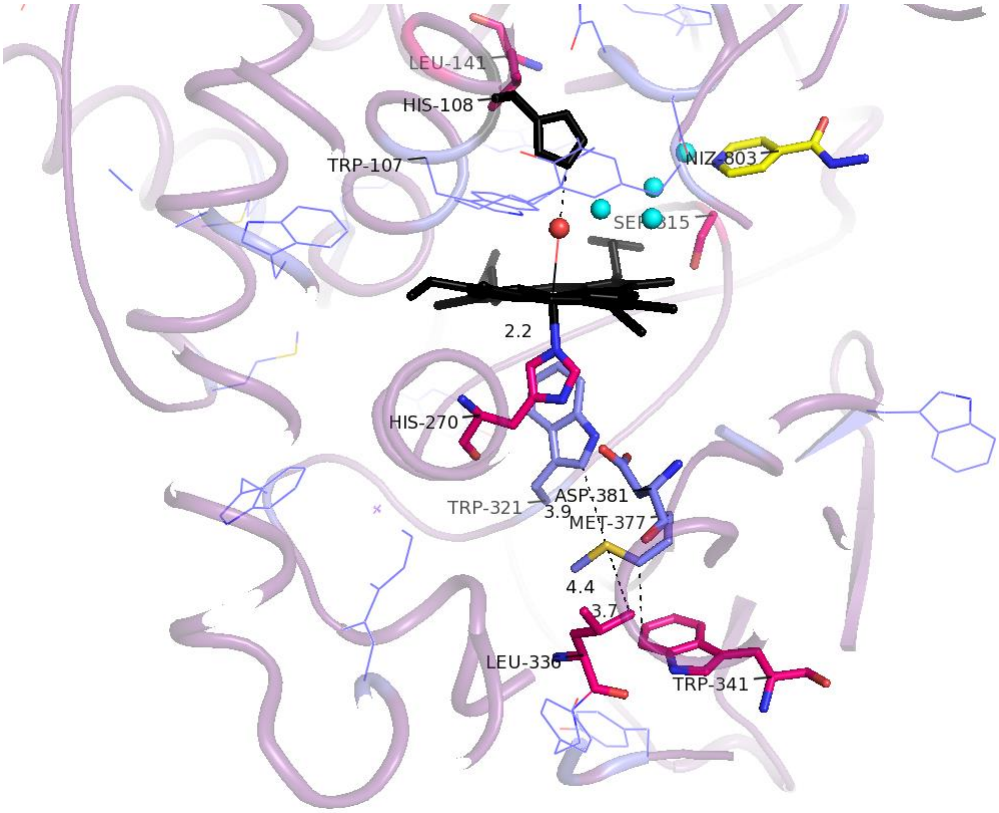
LEU-141
HIS-108
TRP-107
NIZ-803
SER-315
2.2
HIS-270
TRP-321
ASP-381
3.9
MET-377
4.4
3.7
LEU-330
TRP-341

B

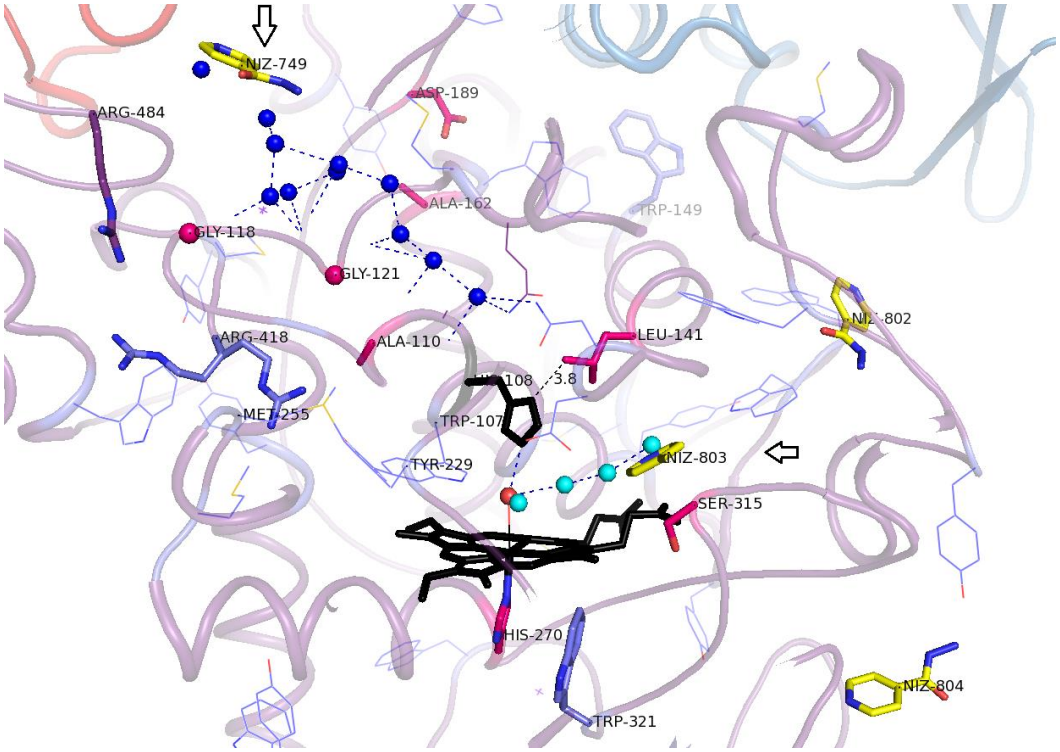
NIZ-749
ARG-484
ASP-189
ALA-162
TRP-149
GLY-118
GLY-121
ARG-418
ALA-110
LEU-141
3.8
MET-255
TRP-107
TYR-229
NIZ-803
SER-315
HIS-270
TRP-321
NIZ-804

Figure 2